DDX31: A Novel Functional Oncogene Promotes Migration and Proliferation of Pancreatic Cancer

Yang Liu
Tianjin Medical University Cancer Institute and Hospital: Tianjin Tumor Hospital
Yongjie Xie
Tianjin Medical University Cancer Institute and Hospital: Tianjin Tumor Hospital
Jinsheng Ding
Tianjin Medical University Cancer Institute and Hospital: Tianjin Tumor Hospital
Liangliang Wu (wuliangliang830906@126.com)
Tianjin Medical University Cancer Institute and Hospital: Tianjin Tumor Hospital https://orcid.org/0000-0001-5611-2704

Research Article

Keywords: DDX31, pancreatic cancer, EMT, migration, proliferation

Posted Date: June 7th, 2021

DOI: https://doi.org/10.21203/rs.3.rs-520114/v1

Abstract

Purpose: Pancreatic cancer is one of the most malignant cancers with rapid disease progression. Pancreatic ductal adenocarcinoma (PDAC) accounts for more than 90% in exocrine pancreatic cancer. DDX31 is one of the Asp-Glu-Ala-Asp (DEAD)-box RNA helicases (DDX) family member, which has never been reported in pancreatic ductal adenocarcinoma. Through comprehensive analysis of bioinformatics screening, clinical pathological data and experiment results verification, we found DDX31 may be a promising oncogene.

Patients and methods: The potential correlation between DDX3 expression and clinical feature of PDAC was analyzed, which revealed that patients with high DDX31 expression may have a poor prognosis. Elevated expression levels of DDX31 in PDAC compared with adjacent normal tissues were determined by immunohistochemical and Western blot analyses. Western blot analysis of N-cadherin, Snail, transwell, and wound healing assays was carried out to evaluate the pro-metastasis effects of DDX31 in PDAC. In vitro experiments included colony formation assay. Edu labeling assay, CCK-8, western blot analysis of Ki67, PCNA, and an in vivo subcutaneous mouse model were used to analyze the role of DDX31 in PDAC proliferation.

Results: In our research, integrated bioinformatics analysis of the TCGA and GEO databases was performed to identify the metastasis and proliferation-related differentially expressed genes (DEG). DDX31 predicts strong metastasis and proliferation capacity of PDAC, was finally screened. Then, the clinical data identified that highexpression-DDX31 was correlated with pancreatic tumor size, pathological grade, and lymph node metastasis. The in vitro and vivo experiments revealed that overexpression-DDX31 promoted the migration, proliferation and cell viability of pancreatic cancer cells, these functions of DDX31 had also been proved in the knockdown results. Moreover, the EMT related markers and proliferation markers were identified to be positively regulated by DDX31 in pancreatic cancer cells.

Conclusion: Thus, our work uncovered that DDX31 promotes migration and proliferation in PDAC and might be a promising therapeutic target in pancreatic cancer.

Introduction

The 5-year survival rate of pancreatic cancer (PC) is less than 8%. It is a highly malignant cancer that is hard to treat and diagnose early[1]. The most common type of PC is pancreatic ductal adenocarcinoma (PDAC); it counts for > 90% in exocrine PC[2]. For most patients with PDAC, the tumor has metastasized already when they are diagnosed, and majority of patients with PDAC have lost the chance to seek radical surgery treatments. Thus, effective biomarkers for early diagnosis and new therapeutic targets for PC are urgently needed.

Nowadays, increasingly updated available databases and web-based tools are utilized to provide more reliable bioinformatics methods to identify some valid biomarkers for PC. Cellular proliferation and EMT are known to contribute to cancer progression, metastasis, and other malignant behaviors[3]. Differentially expressed gene (DEG) analysis is conducted in mRNA profile datasets of the GEO and TCGA databases by bioinformatic methods. Furthermore, increasingly updated available databases and web-based tools provide us with more reliable and valuable insights to identify some valid biomarkers for PC. Comprehensive analysis of DEG screening based on mRNA profiles from paired pancreatic tumor tissues and normal tissues and single cell RNA sequencing of tumor tissues from KPC (LSL-Kras; LSL-Trp53; Pdx-1-Cre) mice have been conducted to identify DDX31 as the targeted gene.

Members of the Asp–Glu–Ala–Asp (DEAD)-box RNA helicase (DDX) family first emerged as RNA helicases correlated with RNA metabolism. The critical functions related to DDX family members in bacteria and archaea have been revealed in few studies[4]. Parts of the DDX family members can bind to other important nuclear proteins by the ATP-dependent

pathway to form large complexes and then perform additional functions in the cytoplasm and nucleus[5]. Elevated expression of some DDX family members has been found in some types of cancer in early studies[6]. Some of them play an important role in cancer cells including promoting cell proliferation, invasion, and other tumor biological behaviors. Recently, DDX31 was found to play a vital role in promoting migration and invasion in muscle-invasive bladder cancer[7]. In the present study, through multiple database screening and comprehensive analysis, we first reveal its clinical significance and action of promoting tumorigenesis and metastasis in PDAC.

Material And Methods

1. Comprehensive screening of DEG expression

The gene expression profile of GSE129455 was downloaded from the Gene Expression Omnibus (GEO) database (http://www.ncbi.nlm.nih.gov/geo/). The mRNA profiles of pancreatic tumors and adjacent normal tissues were generated by high-throughput sequencing based on GPL11154 Illumina HiSeq 2000 (*Homo sapiens*). Ten paired tumor and normal tissues were obtained (GSE119794). Specifically, DEGs were identified from gene expression profiles of tumor tissues and matched normal tissues. We utilized the KPC SCRNAseq (single cell RNA sequencing) datasets containing 7,500 cells from four KPC mice enriched with fibroblast and ductal cell populations and downloaded from GEO databases (GSE129455)[8] to analyze the differential expression of genes between ductal and acinar cells.

2. Correlation analysis

Correlation analysis was conducted between the 73 candidate genes and EMT-related markers as well as proliferative markers in the mRNA profile based on 161 PC samples of TCGA database. The prognostic and valuable markers that were highly correlated with these markers (CDH2/SNAIL/Ki67) compared with other candidate genes were identified via Spearman correlation analysis.

3. Gene set enrichment analysis (GSEA) in PC tissues from the TCGA database

A total of 161 PC samples were downloaded from the TCGA databases and divided into two groups based on DDX31 expression level. Gene set enrichment analysis (GSEA)[9] in PC tissues was conducted in accordance with the mRNA expression level of DDX31. We filtered significantly differential enriched pathways on the basis of the P-value threshold, and the absolute value of $p < 0.05$ was considered to represent a significant difference.

4. KEGG and GO pathway enrichment analysis

The differentially co-expressed profiles of mRNAs in three datasets were studied via GO and KEGG enrichment analysis using the online software Metascape (http://metascape.org/)[10].

5. Human tissue specimens and immunohistochemical (IHC) analysis

We were allowed by the Ethics Committee of the Tianjin Cancer Institute and Hospital (Tianjin, China) to acquire the paraffin sections of four patients. These 86 patients received radical pancreaticoduodenectomy from January 2017 to September 2020. We randomly selected the clinical patients who had been diagnosed as TNM3, TNM2 and TNM1. IHC of DDX31 was performed in these 86 cases of tumor tissues and matched normal pancreas tissues. Fourteen cases of fresh clinical tumor and normal pancreas tissue samples were collected to identify the expression of DDX31 by Western blot. IHC analysis of the PDAC tissue for DDX31 (NOVUS; NBP1-21322, 1:400) was performed using a DAB substrate kit (ORIGENE, ZLI-9019). Three representative fields of pancreatic cancer tissues IHC stain (100×, 200× magnification) and

representative paired normal and tumor tissues IHC stain (100×, 200× magnification) were evaluated under a light microscope.

6. Cell culture and reagents

Human PC cell lines BxPC-3, MIA-PaCa2, SW1990 and L3.7 were purchased from ATCC (Rockville, MD). All PC cell lines were cultured in 37 °C in a 5% CO_2 incubator. PC cell lines were cultured in RPMI-1640 medium and DMEM (GIBCO) with 10% fetal bovine serum (FBS).

7. Plasmid construction and cell transfection

DDX31 overexpression in PC cell lines and lentivirus-mediated plasmid was conducted using the pCDH-cDNA system (Biosettia) following the manufacturer's instructions. Lentiviruses were produced in 293T cells for the stable transfection of the cell lines. Human DDX31 cDNA was cloned into a pCDH plasmid expression vector (pCDH-DDX31), and pCDH vector was used as control. Stable cell lines were generated using puromycin. The efficiency of overexpression was confirmed by Western blot.

The stable knockdown PC cell lines, shRNA was designed by the Biasatti's website (http://biosettia.com/support/shrna-designer). PLVi-shRNA-bsd vectors were purchased from Biasatti company, three shRNA sequences for DDX31 were synthesized and cloned into the plasmid. Detailed information of the shRNA sequence for DDX31 were listed in the supplementary table1. The most effective one was used for the next experiments, the effective of the three shRNA have been identified by western blot.

8. Wound healing assay

Wound healing assay was performed with 6-well plates (Corning, 3516). On the first day, BxPC-3 and MIA-PaCa2 cells were counted and seeded in 6-well plates (5×10^5 cells per well). On the second day, when the cellular confluence was almost 100%, we used a pipette tip to draw a straight line on the bottom of plates. Cell migration was observed under a microscope. This experiment was conducted for at least three times. Random fields of each independent experiment were collected under a light microscope. The area of the wound was measured by Image-J (National Institutes of Health).

9. Transwell migration assay

In this study, 8.0 μm pore plates (Corning, 3422) were used to perform migration assay. In brief, 5×10^4 cells were added to the upper chamber of a transwell membrane with DMEM or 1640. DMEM or 1640 with 10% FBS was added to the lower chamber, and the cells were incubated for 18 h. Cells that had migrated to the bottom of the filter were stained with Giemsa stain purchased from Beijing Solarbio Science & Technology Company (SOLARBIO, G1020). All experiments were repeated independently for at least three times. For microscopy analysis, three random horizons were selected for cell counting.

10. Western blot analysis

Cell extracts were prepared by SDS lysis buffer mixed with proteinase inhibitor cocktail (Sigma). The protein concentrations were detected by protein assay kit (Thermo). Protein samples were separated by SDS-PAGE, and the target proteins were detected by Western blot analysis with the antibodies to DDX31 (NOVUS; NBP2-92273, 1: 1000), N-cad (Cell Signaling Technology; 13116s, 1:1000), Snail (Cell Signaling Technology; 2879s, 1:1000), Ki67 (Abcam; ab92742,1:1000), PCNA (Abcam; ab95225, 1:500), and β-Tubulin (Beijing Ray Antibody Biotech; RM2003, 1:5000).

11. Immunofluorescence imaging

Cell suspensions (2×10^4) were plated into 24-well plates (Corning, 3738) in each chamber and allowed to adhere for at least 12 h. Concentrations of antibody to DDX31 (NOVUS; NBP2-92273) were confirmed as 1:500 via immunofluorescence staining. The MIA-PaCa2 and SW1990 cells were incubated with anti-DDX31 antibodies at 4 ℃ overnight. Then, the cells were incubated with Alexa Fluor488-conjugated goat polyclonal anti-Rabbit IgG (Thermo, A11034) at room temperature for 1 hour. DAPI Fluor mount-G media with DAPI nuclear stain (Southern Biotech, 0100-20) was used to identify nuclei. Immunostaining and imaging were carried out by using a microscope (200× magnification).

12. Colony formation assay

Cell growth was assessed via colony formation assay. In brief, 10^3 cells were seeded in each well with a 6-well plate. After 14 days, the cell clones were stained by crystal violet. Cell fixation reagents were purchased from Beijing Solarbio Science & Technology Company. The clone number was counted by Image-J (National Institutes of Health). Every experiment was repeated at least three times.

13. Edu stain assay

The cell proliferation level was tested by EdU Apollo®567 In Vitro Imaging Kit (Ribo Bio, China, C10731-1). Cells were seeded into 96-well plates at 8×10^3 cells/well and incubated overnight, then 5-ethynyl-20-deoxyuridine (EdU) with a final concentration of 50 mM was added into the media and the plates were incubated at 37 ℃ for 2 h. All procedures were performed according to the manufacturer's protocol. Three random fields of each well were chosen and observed under fluorescence microscopy. All images were processed using Image J software and the proportion of EdU incorporated cells was calculated. Three independent experiments were performed for quantification.

14. Cell viability assay

PC cells were plated in a 96-well plate (Corning, 7605), and about 2000 cells were plated in each well. Four 96-well plates were plated at the same time; one was used for baseline, and the other plates were cultured for 24, 48, and 72 h. CCK-8 reagents (Bimake, B34302) were added into each well for 2 h and incubated at 37 ℃. The absorbance was examined by a microplate system at 450 nm. Each group was established with at least three holes, and each experiment was repeated three times.

15. Animal studies in the subcutaneous PC mouse model

Female 5-week-old nude NU/NU mice were purchased from SiPeiFu Biotechnology Company. All these mice were maintained in a barrier facility on HEPA-filtered racks. All animal studies were conducted under an approved protocol[11]. Tumor cells were harvested by trypsinization, washed with ice PBS, and resuspended at 1×10^7 cells per milliliter in PBS. Subsequently, 1×10^6 cells were used to establish every subcutaneous xenotransplant tumor model of human PC in nude mice. In the log phase, BxPC-3 was implanted subcutaneously in nude mice and observed 3 times a week.

16. Statistical analysis

Statistical analysis was performed with GraphPad Prism version 8.0 (San Diegl, CA, USA) and SPSS version 26.0 (IBM SPSS, Armonk, NY, USA). Each experiment was conducted in triplicate, and data were presented as the mean ± SD unless otherwise stated. The variance between the groups was statistically compared. Student’s t test was conducted to compare the mean values. The correlations between DDX31 expression level and patients’ survival time after surgery

was performed by Kaplan–Meier method. The categorical data were analyzed by Chi-square test. *p<0.05, **p<0.01, ***p< 0.001, ****p< 0.0001 indicated significant differences, and NS meant nonsignificant.

Results

1. Comprehensive screen of vital DEGs in PC

The general data analysis and experiment designs are shown in Fig. S1. A total of 73 candidate genes were screened through three public databases. Log fold change (FC) and P-value were used to select differentially expressed mRNAs among three variable datasets. We selected DEGs according to the P-value threshold and absolute value of FC. A value of $p < 0.05$ was considered to represent a significant difference. We performed UMAP analysis, and cell types with the mRNA expression matrix of 7500 cells were identified based on specific markers of different cell clusters (Fig. 1A and Table 2). A total of 1824 genes that were significantly upregulated in ductal cells were selected compared with the acinar cells in the four KPC mice datasets (Fig. 1B). We downloaded PDAC samples from the TCGA database and divided them into the H-EMT and L-EMT groups based on the mRNA expression level of CDH2 (higher than 75% of CDH2 expression was defined as the H-EMT group and lower than 25% of CDH2 expression was defined as the L-EMT group). DEG analysis demonstrated that 1823 genes were upregulated in the H-EMT group. The DEGs with significant differential expression were shown in a heatmap between the H-EMT group and L-EMT group (Fig. 1C). Ten paired tumor and normal tissues were also subjected to DEG analysis, and results were displayed in a volcano plot (1051 genes were upregulated; Fig. S2). All the co-expressed DEGs were represented with a Venn diagram (Fig. 1D), and 73 candidate genes were selected (Table 3).

2. Correlation analysis and GSEA analysis of DDX31-related enrichment gene sets

To determine the target gene for future research, we conducted correlation analysis between the 73 candidate genes and EMT-related markers and proliferative markers in the mRNA profile (Fig. 2A). Finally, DDX31 was screened as the prognostic and valuable marker, which was much strongly correlated with these markers (CDH2/SNAIL/Ki67) compared with other candidate genes (Fig. 2A-2B). To further determine the molecular mechanisms and potential functions of DDX31 in PC development, the expression matrix of 161 PDAC samples was downloaded from the TCGA databases and divided into two groups, namely, DDX31 expression level higher than 75% and lower than 25%. GSEA in PC tissues was conducted on the mRNA expression level of DDX31. We filtered significantly differential enriched pathways based on the P-value threshold, and the absolute value of $p < 0.05$ was considered to represent a significant difference (Table 4). Finally, we noted enrichments of gene sets including adherens junction, focal adhesion, PC, and pathway in cancer in the tissues with high DDX31 expression (Fig. 2C).

3. DDX31 might be a potential oncogene in PC

To investigate the expression of DDX31 in PDAC specimens, we performed IHC analysis in 86 tumor tissues and paired normal pancreas tissues (Fig. 3A-3B), 14 paired tumor tissues and normal fresh pancreatic tissues were picked randomly to do western blot analysis (Fig. 3C-3D). We found that the expression of DDX31 increased in tumor tissues. The 86 tumor tissues were divided into two groups according to the expression of DDX31: DDX31-Low (DDX31 weak expression and moderate expression) and DDX31-High (Fig. 3E). According to the results of correlation analyzing of DDX31 expression and patients clinicopathological features, we found that the high-expression of DDX31 was strongly related with the tumor size (c^2=3.9681, p=0.0464), Lymph node metastasis (c^2=9.9801, p=0.0016), TNM grade (c^2=5.8091, p=0.0159) of PDAC patients and tumor tissues' histological grade (c^2=4.3641, p=0.0369) (Table 5). At the same time, the Kaplan-Meier analysis of TMA data uncovered that DDX31-high expression patients had significant low overall survival rate (OS) and progression-free survival rate (PFS) compared with low-expressed (weak expression and

moderate expression) of DDX31 group patients (Fig. 3E-3F). Next, univariate and multivariate analysis of clinical follow-up data of PDAC patients were performed, the results indicates that the expression of DDX31 correlated with OS and PFS in PDAC patients (Table6). Together, our results indicates that high expression of DDX31 has a great important prognostic value in PDAC development and is an independent risk factor for PDAC progression.

In addition, we found that most PDAC cell lines showed higher protein expression of DDX31 than that in the immortalized normal ductal epithelial cell line HPDE6c7 (Fig. S3A). MiaPaca-2 with low endogenous expression of DDX31 and SW1990 with high endogenous expression of DDX31 were chosen to confirm the cellular location of DDX31 in PC cells (Fig. S3B). The results of immunofluorescence analysis revealed that DDX31 was mainly localized to the nucleus in PC cells.

4. DDX31 promoted PC cellular migration

To explore the potential roles of DDX31 in PC cells, we performed loss and gain-of-function studies. According to the results of Western blot in Fig. S3A, BxPC-3 and MIA-PaCa2 cell lines were chosen for subsequent studies. BxPC-3-vector/DDX31-OE and MiaPaca-2-vector/DDX31-OE cell lines were established, and related functional experiments were performed to elucidate the role of DDX31 in PDAC. First, the protein expression levels of DDX31 in BxPC-3-vector/DDX31-OE and MiaPaca-2-vector/DDX31-OE cell lines were validated by Western blot. To determine the role of DDX31 in cellular migration, wound healing assay and transwell migration assay were performed. Wound healing assay was conducted to verify the effect of DDX31 overexpression on PC cell (BxPC-3/ MIA-PaCa2) mobility (Fig. 4A-4B). Compared with the WT PC cells and vector control PC cells, overexpression of DDX31 significantly promoted cells' wound closure. The results of transwell assay also showed that the migration rate of PC cells significantly increased upon DDX31 overexpression (Fig. 4B).

Given that DDX31 was highly expressed in SW1990 cells and L3.7 cells. Sh-DDX31 was transfected into these two cell lines. Next, we focused on the effects of knock down DDX31 on cellular mobility capacities in SW1990 and L3.7 cell lines. In contrast, the opposite experiment results were obtained in knockdown-DDX31 PC cell lines. As shown in Fig. 4C-4D, according to the results of transwell assay, wound-closing procedure, depletion of DDX31 significantly decreased the capacity of cellular migration.

5. DDX31 promoted cellular proliferation and cell viability in PC cells

Crystal violet staining was carried out to evaluate the clone formation ability between DDX31-overexpressing PC cells (BxPC-3/ MIA-PaCa2) and vector control (including WT control) (Fig. 5A). The DDX31-overexpressing PC cell lines demonstrated a greater number of colonies than the vector control as well as WT control. Edu staining assays were also performed. As shown in Fig. 5B, PC-DDX31-OE showed a higher percentage of Edu-positive cancer cells. Interestingly, DDX31 overexpression led to an increased cell proliferation capability in the DDX31-OE PC cells (BxPC-3/ MIA-PaCa2) compared with WT-CTRL/pCDH-VEC control group. In addition, the effect of DDX31 overexpression on human PC cell viability was detected by CCK-8 assay. Considering the results, overexpression of DDX31 promoted the cell vitality of BxPC-3 and MIA-PaCa2 cells (Fig. 5C).

For further confirming the proliferation oncogene function of DDX31, the DDX31-knockdown PC cells (SW1990/L3.7) were constructed subsequently. Clone formation and EdU stain assay revealed downregulation of DDX31 regressed the proliferation of PC cells (Fig. 5D-5E). Otherwise, to explore the effects of DDX31 knockdown on cellular vitality, we carried out CCK-8 test. The cell viability was detected when the cell began adhere growth 0h, 24h, 48h, 72h. At 72h, the downregulation of DDX31 obviously inhibited the cell viability of PC cells compared with scramble group and WT PC cells (Fig. 5F).

To further identify the role of DDX31 in PDAC proliferation, in vivo subcutaneous tumor models were used. Subcutaneous tumors in nude mice and isolated tumors after 19 days and 5 days formed by BxPC-3 infected with pCDH-DDX31, pCDH-VECTOR lentivirus and WT-CTRL PC cell lines. As shown in Fig. 5G, consistent results revealed that overexpression of DDX31 significantly promoted tumor growth.

6. DDX31 positively regulated EMT and proliferation markers.

To identify the results of correlation analysis and explore the mechanism by which DDX31 promotes PC cell migration and proliferation, we performed Western blot with some confirmed EMT-related proteins and proliferation-related protein antibodies. As shown in Fig. 6, the proteins N-cadherin, Snail, ZEB1, Ki67, and PCNA were positively correlated with DDX31 OE-expression (Fig. 6A). The opposite results were observed in knockdown-DDX31 PC cells (Fig. 6B). These results revealed that DDX31 positively regulated the migration and invasion of PC cells through these classical EMT and proliferation markers.

Discussion

DEAD family members have attracted increasing attention in recent years, and their functions in cancer pathogenesis and development were reported in recent and previous studies. DDX1[12], DDX2[13], DDX5[14], DDX6[15], DDX9[16], DDX43[17], DDX48[18], DDX53[19], and DDX56[20] have been reported in neuroblastoma and retinoblastoma, melanoma hepatocellular carcinoma colorectal cancer, lung cancer, and gastric cancer. However, their functions in PC have never been reported and remain unclear. In our study, we first focused on DDX31 involved in EMT and proliferation and explored their expression and prognostic value in PC. DDX31 was found to be highly expressed in PC. Furthermore, DDX31 showed upregulated expression of EMT-related markers in PC, and it was proven to promote the invasion and migration of PC cells in vitro in our study. These discoveries suggested that DDX31 played important roles in the progression of PC, but its function has not been explored. Our clinical data statistics indicated that DDX31 was upregulated in PC and DDX31 was a marker associated with invasive prognosis in PC. Moreover, GO/KEGG enrichment analysis was conducted, and we observed in patients with TCGA that the expression of DDX31 was positively correlated with proliferation and EMT. Moreover, DDX31 expression was significantly positively correlated with RNA, DNA transportation, and degradation in the nucleus. Through analysis in the cBioportal database, we identified amplification as one of the main mechanisms by which DDX31 is upregulated in PC. To confirm more potential mechanisms of DDX31 in PC progression, we conducted GSEA analysis in PC tissue from the TCGA database and found that upregulated expression of DDX31 might promote PC progression by promoting the adhesion and proliferation of PC cells. To further validate its function, we performed functional experiments after overexpressing DDX31 in BxPC-3 and MIA-PaCa2 cell lines and knockdown-DDX31 in SW1990 and L3.7 to verify the function of DDX31 in PC transfected with lentivirus. We verified that the EMT markers (N-cadherin and Snail) and proliferation-related markers (Ki67 and PCNA) were positively regulated by DDX31 (Fig. 6). These results indicated that DDX31 could promote the migration and invasion of PC cells may through regulates these classical proteins. IHC and Western blot technology revealed that DDX31 significantly increased in PDAC tissues compared with that in adjacent normal tissues. We further validated that DDX31 was mainly localized to the nucleus in PC cells as shown in the immunofluorescence image and results of GO enrichment analysis. We then performed CCK8 and EDU assays to explore its function in vitro. The results showed that overexpression of DDX31 significantly promoted tumor growth compared with the control group. Our study demonstrated the abnormal expression and prognostic values of DDX31 in PC. In addition, we highlighted the association between DDX31 and the proliferation, invasion, and migration of PC cells. Combine its clinical links with OS and PFS, DDX31 might be a valuable biomarker for the diagnosis, therapy, and prognostic prediction of patients with PC. More significant importance should be further connected to DDX31 in future studies on PC, and further explorations into deep molecular mechanisms are worth conducting. DDX5 regulates PDGF-induced EMT[21], and DDX5/DDX17

modulates cell migration through NFAT5 regulation in colon cancer cells. DDX31 silencing can induce p53-dependent G1 arrest and subsequent apoptosis in renal cell carcinoma[22]. In muscle-invasive bladder cancer (MIBC), nuclear DDX31-bound mutp53/SP1 enhances mutp53 transcriptional activation, which results in the migration and invasion of MIBC[7]. The mechanism by which DDX31 promotes EMT and the proliferation of PDAC needs further exploration. In addition, four alternative splice variants of DDX31 have been confirmed. In our study, only one of them was focused on, and the others remain to be studied.

Conclusions

In summary, our research found that DDX31 was significant oncogene to promote pancreatic cancer cells migration and proliferation, its' protein expression predicted a poor prognosis in pancreatic cancer and might be a vital therapy target for pancreatic cancer.

Abbreviations

DDX31, DEAD-Box RNA helicases; PC, pancreatic cancer; PDAC, pancreatic ductal adenocarcinoma; EMT, Epithelial Mesenchymal Transition; DEG, Differentially expressed gene; TCGA, The Cancer Genome Atlas; GEO, Gene Expression Omnibus; SC-RNAseq, single cell RNA sequencing; GSEA, Gene set enrichment analysis; CCK-8, cell counting kit-8; PCNA, Proliferating cell nuclear antigen; ZEB1, Zinc- finger E-box Binding homeobox-1.

Declarations

Acknowledgments

Yang Liu provide the main idea and experiments design of this project. Yongjie Xie, Jinsheng Ding performed the bioinformatics data analysis. Liangliang Wu given the main supplementary research idea. All the authors participated the manuscript composition. Thanks for their works in this research.

Disclosure

The author reports no conflicts of interest in this work.

Ethics committee approval

The utilization of the specimens and patients' information were approved by the Ethics Committee of the Tianjin Medical University Cancer Institute and Hospital (Tianjin, China). All patients provided written consent for the use of their samples and diseases information for further study according to the ethics committee and in accordance with recognized ethical guidelines of Heisinki.

Funding source

This research work was favored by the National Natural Science Foundation of China (81572372); National key R&D Program of China (NO. 2016YFC1303202) and National key research and development program "precision medicine research" program (NO.2017YFC0908300).

References

1. Balachandran VP, Beatty GL, Dougan SK. Broadening the Impact of Immunotherapy to Pancreatic Cancer: Challenges and Opportunities [J]. Gastroenterology, 2019, 156(7): 2056-2072.
2. Fenocchio E, Filippi R, Lombardi P, et al. Is There a Standard Adjuvant Therapy for Resected Pancreatic Cancer? [J]. Cancers (Basel), 2019, 11(10):
3. Thiery JP, Acloque H, Huang RY, et al. Epithelial-mesenchymal transitions in development and disease [J]. Cell, 2009, 139(5): 871-890.
4. Linder P, Jankowsky E. From unwinding to clamping - the DEAD box RNA helicase family [J]. Nat Rev Mol Cell Biol, 2011, 12(8): 505-516.
5. Jankowsky E. RNA helicases at work: binding and rearranging [J]. Trends Biochem Sci, 2011, 36(1): 19-29.
6. Abdelhaleem M. Over-expression of RNA helicases in cancer [J]. Anticancer research, 2004, 24(6): 3951-3953.
7. Daizumoto K, Yoshimaru T, Matsushita Y, et al. A DDX31/Mutant-p53/EGFR Axis Promotes Multistep Progression of Muscle-Invasive Bladder Cancer [J]. Cancer Res, 2018, 78(9): 2233-2247.
8. Elyada E, Bolisetty M, Laise P, et al. Cross-Species Single-Cell Analysis of Pancreatic Ductal Adenocarcinoma Reveals Antigen-Presenting Cancer-Associated Fibroblasts [J]. Cancer discovery, 2019, 9(8): 1102-1123.
9. Subramanian A, Tamayo P, Mootha VK, et al. Gene set enrichment analysis: a knowledge-based approach for interpreting genome-wide expression profiles [J]. Proc Natl Acad Sci U S A, 2005, 102(43): 15545-15550.
10. Zhou Y, Zhou B, Pache L, et al. Metascape provides a biologist-oriented resource for the analysis of systems-level datasets [J]. Nat Commun, 2019, 10(1): 1523.
11. Zhao T, Jin F, Xiao D, et al. IL-37/ STAT3/ HIF-1alpha negative feedback signaling drives gemcitabine resistance in pancreatic cancer [J]. Theranostics, 2020, 10(9): 4088-4100.
12. Bléoo S, Sun X, Hendzel MJ, et al. Association of human DEAD box protein DDX1 with a cleavage stimulation factor involved in 3'-end processing of pre-MRNA [J]. Mol Biol Cell, 2001, 12(10): 3046-3059.
13. Causevic M, Hislop RG, Kernohan NM, et al. Overexpression and poly-ubiquitylation of the DEAD-box RNA helicase p68 in colorectal tumours [J]. Oncogene, 2001, 20(53): 7734-7743.
14. Cho B, Lim Y, Lee DY, et al. Identification and characterization of a novel cancer/testis antigen gene CAGE [J]. Biochemical and biophysical research communications, 2002, 292(3): 715-726.
15. Godbout R, Squire J. Amplification of a DEAD box protein gene in retinoblastoma cell lines [J]. Proc Natl Acad Sci U S A, 1993, 90(16): 7578-7582.
16. Martelange V, De Smet C, De Plaen E, et al. Identification on a human sarcoma of two new genes with tumor-specific expression [J]. Cancer Res, 2000, 60(14): 3848-3855.
17. Nakagawa Y, Morikawa H, Hirata I, et al. Overexpression of rck/p54, a DEAD box protein, in human colorectal tumours [J]. Br J Cancer, 1999, 80(5-6): 914-917.
18. Squire JA, Thorner PS, Weitzman S, et al. Co-amplification of MYCN and a DEAD box gene (DDX1) in primary neuroblastoma [J]. Oncogene, 1995, 10(7): 1417-1422.
19. Stevens SW, Ryan DE, Ge HY, et al. Composition and functional characterization of the yeast spliceosomal penta-snRNP [J]. Mol Cell, 2002, 9(1): 31-44.
20. Wei X, Pacyna-Gengelbach M, Schlüns K, et al. Analysis of the RNA helicase A gene in human lung cancer [J]. Oncology reports, 2004, 11(1): 253-258.
21. Yang L, Lin C, Liu ZR. P68 RNA helicase mediates PDGF-induced epithelial mesenchymal transition by displacing Axin from beta-catenin [J]. Cell, 2006, 127(1): 139-155.

22. Fukawa T, Ono M, Matsuo T, et al. DDX31 regulates the p53-HDM2 pathway and rRNA gene transcription through its interaction with NPM1 in renal cell carcinomas [J]. Cancer Res, 2012, 72(22): 5867-5877.

Tables

Table 1 shRNA sequences for stable knockdown cell lines

Human DDX31 shRNA1	CCGGCCCTTCAAGCAATGGAGTCAACTCGAGTTGACTCCATTGCTTGAAGGGTTTTTG
Human DDX31 shRNA2	CCGGGGACATCACAGTGATACTTAACTCGAGTTAAGTATCACTGTGATGTCCTTTTTG
Human DDX31 shRNA3	CCGGGCTGAAATCCTACGTTCGGAACTCGAGTTCCGAACGTAGGATTTCAGCTTTTTG

Table 2 Cell cluster markers

Cell types	**Markers**
Macrophage	Apoe Saa3 C1qc
Neutrophils	S100a8 S100a9 G0s2
Ductal cells	Clu Krt18 Krt8 Krt19 Krt7 Epcam Tff1
EMT-like cells	Cdkn2a S100a6 Igfbp4 Vim Spp1
Dendritic cells	Ccl5 Cd34 Ccr7
Fibroblasts	Dcn Col1a1 Col3a1
Endothelial cells	Igfbp7 Plvap Cd34
Acinar cells	Ctrb1 Prss2 Try5

Table 3 73 candidate oncogenes

DEGs	Genes
KPC &GEO& TCGA datasets	TUBA1A CNPY4 VAT1 CBX1 CDH2 SMAD7 SLC39A6 DCLK2 BEND6 MAP1A UBE2E2 ARHGEF17 ATP6AP2 RAB2B WASF1 PHLDB2 MYH10 RBFOX2 BICD2 VIM MXRA7 VASH1 KATNAL1 PTK7 FTO ADAMTS2 MMD PTRF ITGA5 NDST1 TMEM200 ANAV1 MEIS3 TCEAL4 EHD3 CERCAM MSN PRKACA MARCKS KIF3C LAMB1 GNAI2 ANXA6 TIMP2 FADS1 SGTB BBS9 YWHAQ FAM127C ELOVL5 OAZ2 FAP NREP DDX31 EFHA4 ASAP2 WFDC2 ERRFL1 MSLN SAPCD2 BAIAP2 PODH1 GJB4 MAD2L1 USP43 ANXA8 DUSP4 SFN WNT3B PLEK2 DNAJB5 TMX3 ADAM19

Table 4 GSEA in PC tissues based on the mRNA expression level of DDX31.

NAME	SIZE	ES	NES	NOM p-value
KEGG_RNA_DEGRADATION	57	0.61348784	1.780325	0.001949318
KEGG_SNARE_INTERACTIONS_IN_VESICULAR_TRANSPORT	38	0.58324313	1.7738926	0
KEGG_AMINOACYL_TRNA_BIOSYNTHESIS	41	0.63782054	1.7436424	0.007751938
KEGG_UBIQUITIN_MEDIATED_PROTEOLYSIS	133	0.54157966	1.7263068	0
KEGG_RNA_POLYMERASE	29	0.61857345	1.7209494	0.00204918
KEGG_LYSINE_DEGRADATION	44	0.5063957	1.6180567	0.003853565
KEGG_SPLICEOSOME	124	0.5553877	1.6153736	0.02385686
KEGG_BASAL_TRANSCRIPTION_FACTORS	35	0.5407484	1.57773	0.007648184
KEGG_NUCLEOTIDE_EXCISION_REPAIR	44	0.5674203	1.5697331	0.02008032
KEGG_OOCYTE_MEIOSIS	111	0.45195308	1.5587206	0.02268431
KEGG_VALINE_LEUCINE_AND_ISOLEUCINE_BIOSYNTHESIS	11	0.58958447	1.5454466	0.046153847
KEGG_PHOSPHATIDYLINOSITOL_SIGNALING_SYSTEM	76	0.4412696	1.5208397	0.027290449
KEGG_ADIPOCYTOKINE_SIGNALING_PATHWAY	67	0.4224689	1.516984	0.028957529
KEGG_REGULATION_OF_AUTOPHAGY	34	0.42916083	1.5090051	0.040935673
KEGG_PROGESTERONE_MEDIATED_OOCYTE_MATURATION	85	0.44174823	1.5069677	0.01734104
KEGG_MTOR_SIGNALING_PATHWAY	52	0.45748323	1.4917169	0.032882012
KEGG_INSULIN_SIGNALING_PATHWAY	137	0.40029576	1.4715608	0.042471044
KEGG_PURINE_METABOLISM	155	0.3754888	1.4525765	0.025390625
KEGG_WNT_SIGNALING_PATHWAY	149	0.38113543	1.4408966	0.043560605
KEGG_ADHERENS_JUNCTION	73	0.39732743	1.2510679	0.023320158
KEGG_PANCREATIC_CANCER	73	0.39092436	1.2247373	0.043
KEGG_PATHWAYS_IN_CANCER	324	0.30733502	1.1637824	0.0245
KEGG_FOCAL_ADHESION	19	0.22142605	1.14816324	0.02134725

Table 5 Relationships of DDX31 expression and clinicopathological characteristics in 86 patients with PC

	DDX31 expression				
	All	Low	High		
Feature	86	n=47	n=39	c^2	*p*
Age(year)				0.28901	0.5909
<60	48	25	23		
≥60	38	22	16		
Gender				0.53181	0.4658
Male	56	29	27		
Female	30	18	12		
pTNM stage				5.8091	0.0159
	19	15	4		
-	67	32	35		
Histological grade				4.3641	0.0369
G1	20	15	5		
G2/G3	66	32	34		
Tumor diameter				3.9681	0.0464
<5	41	27	14		
≥5	45	20	25		
Lymph node metastasis				9.9801	0.0016
No	49	34	15		
Yes	37	13	24		
Vascular invasion				3.2031	0.0735
No	69	41	28		
Yes	17	6	11		
Nerve invasion				1.1831	0.2768
No	80	45	35		
Yes	6	2	4		

Table 6 Univariate and multivariate analysis of clinicopathological factors for overall survival rate (OS) and progression-free survival rate (PFS)

Features		Univariate analysis			
		OS		PFS	
		HR(95%CI for HR)	*p*	HR(95%CI for HR)	*p*
Sex			0.531		0.629
	Male	1		1	
	Female	1.167(0.720-1.892)		0.876(0.511-1.500)	
Age			0.744		0.86
	<60	1		1	
	>=60	1.080(0.681-1.711)		0.956(0.583-1.570)	
Histological grade			0.02		0.018
	G1	1		1	
	G2/G3	2.626(1.443-4.778)		2.042(1.132-3.684)	
Tumor diameter			0.026		0.15
	<5cm	1		1	
	>=5cm	1.707(1.066-2.734)		1.447(0.875-2.394)	
Lymph node metastasis			<0.001		0.002
	Negative	1		1	
	Positive	2.722(1.642-4.513)		2.266(1.343-3.825)	
Vascular invasion			<0.001		<0.001
	Negative	1		1	
	Positive	3.502(1.958-6.263)		3.164(1.713-5.842)	
Nerve invasion			0.022		
	Negative	1		1	0.199
	Positive	2.768(1.155-6.633)		1.974(0.700-5.570)	
TNM stage			<0.001		<0.001
	I	1		1	
	□	3.844(1.723-8.573)	0.001		
	□	14.390(6.130-33.783)	<0.001	3.275(1.472-7.187)	0.004
DDX31 expression level			<0.0001	9.172(3.869-21.744)	<0.001
	Low expression	1		1	0.003
	High expression	2.337(1.450-3.766)		2.165(1.293-3.624)	

Features		Multivariate analysis			
		HR(95%CI for HR)	*p*	HR(95%CI for HR)	*p*
Vascular invasion			0.038		0.019
	Negative	1		1	
	Positive	2.032(1.040-3.967)		2.324(1.148-4.707)	
TNM stage			<0.001		<0.001
	I	1		1	
	□	4.129(1.810-9.421)	0.001	3.308(1.458-7.501)	0.004
	□	12.196(4.964-29.964)	<0.001	7.038(2.835-17.470)	<0.001
DDX31 expression level			0.022		0.037
	Weekly expression	1		1	
	High expression	1.840(1.090-2.987)		1.764(1.036-3.003)	

Figures

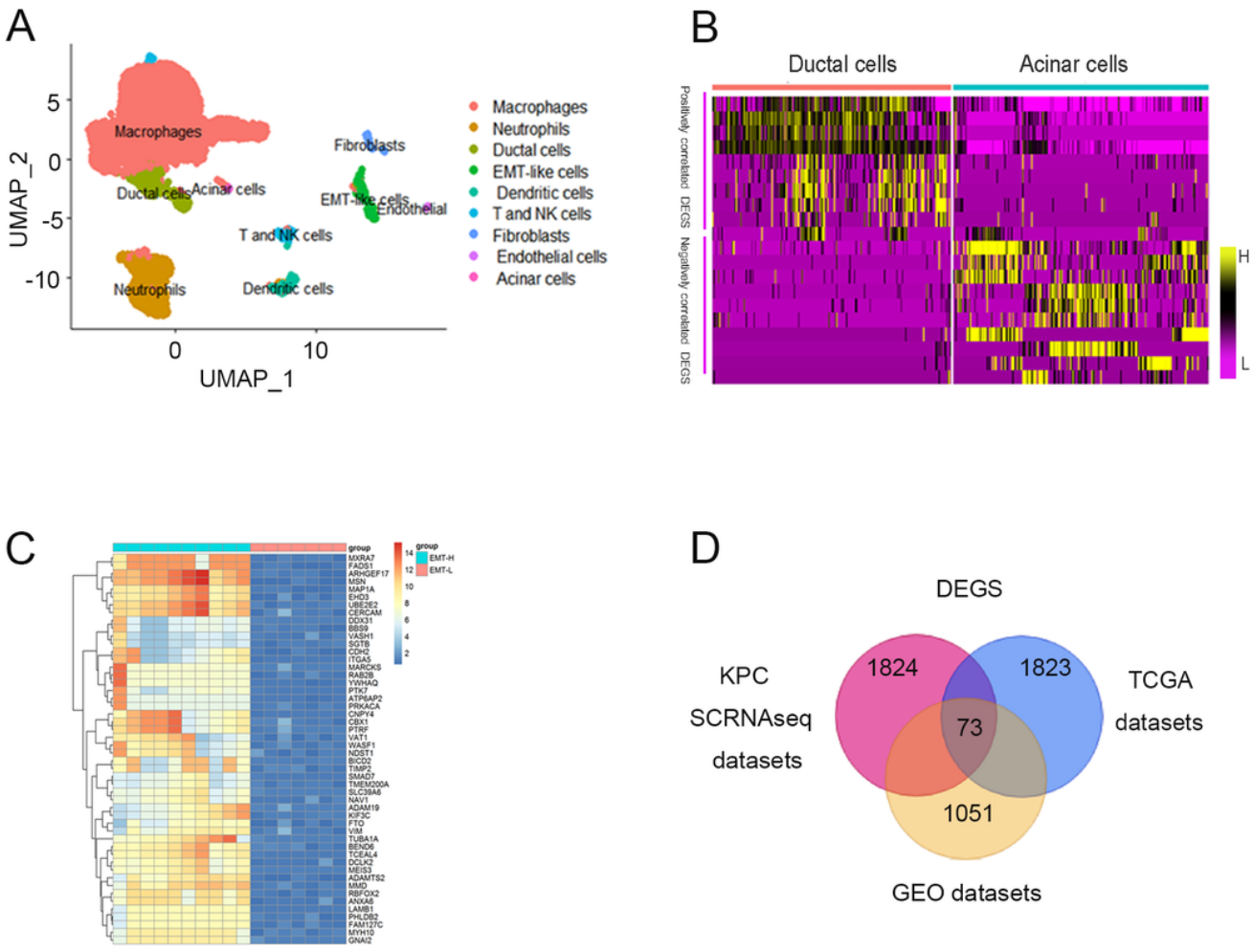

Figure 1

Identification of differentially expressed genes (DEGs) in PC. (A) Single cell RNA sequencing of four KPC mice downloaded from the GEO database (GSE129455). Cell types were represented as a UAMP plot. (B) DEG analysis results are shown as a heatmap between ductal cells and acinar cells. Genes highly expressed and lowly expressed in each part were colored in yellow and purple, respectively. (C) The critical result of DEG analysis between High-EMT and Low-EMT tissues from 161 paired PDAC samples are presented as a heatmap (https://portal.gdc.cancer.gov/). (D) Target genes were obtained by intersecting three databases and shown in a Venn diagram.

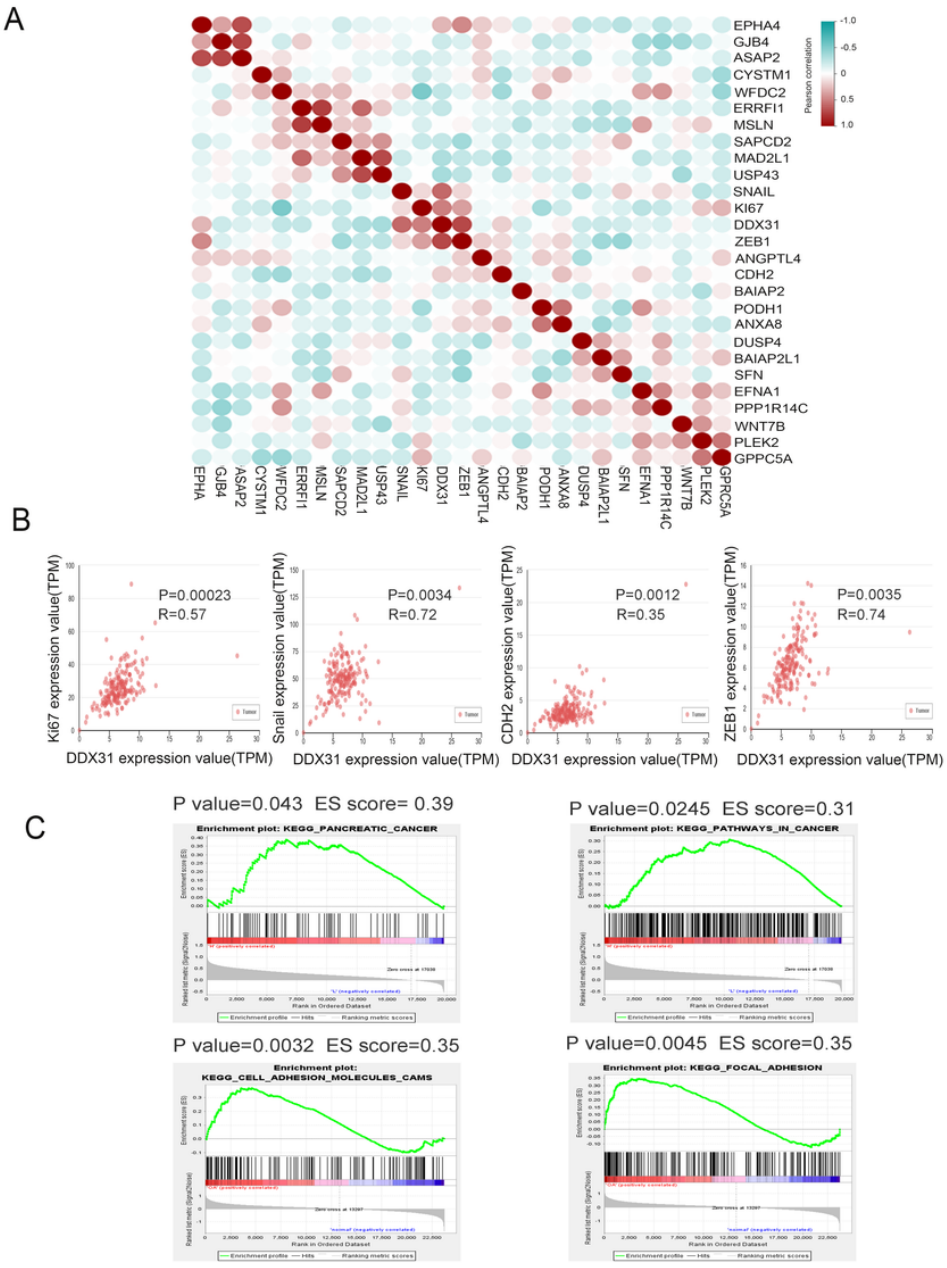

Figure 2

Correlation and GSEA in PC tissues analysis of DDX31. (A–B) DDX31 was positively correlated with proliferative and EMT-related marker (Ki67/CDH2/Snail) mRNA profile expression in PC analysis, especially in PDAC. (C) GSEA analysis of DDX31-related enrichment gene sets: KEGG_PANCREATIC_CANCER (p=0.043; FDR=0.535; Enrichment score=0.366;) KEGG_PATHWAS_IN_CANCER (p=0.0245; FDR=0.412; Enrichment score=0.520;) KEGG_ADHERENS_JUNCTION (p= 0.032; FDR=0.237; Enrichment score=0.440) KEGG_FOCAL_ADHESION (p=0.0045; FDR=0.096; Enrichment score=0.482). GSEA: Gene set enrichment analysis; KEGG: Kyoto Encyclopedia of Genes and Genomes; FDR: False Discovery Rate.

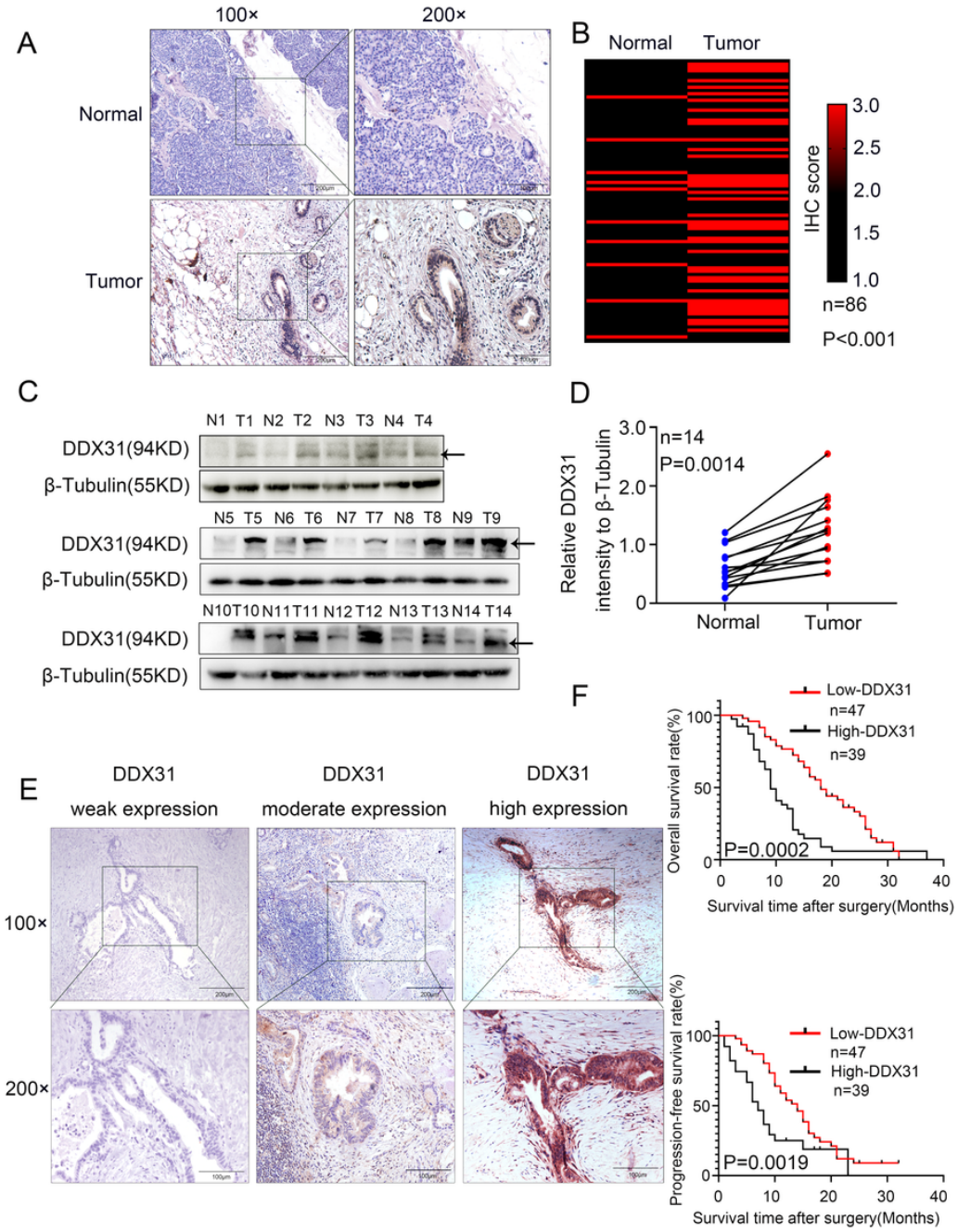

Figure 3

The expression of DDX31 in PDAC tissue and its clinical significance. (A)IHC analysis of DDX31 in pancreatic cancer (×100 and ×200 magnification, Bar = 200 μm and 100μm). (B) The differential expression of DDX31 in 86 normal pancreas tissues and paired tumor tissues is shown in a heat-map and was statistically analyzed by Wilcoxon signed rank tests. (C) Fourteen paired fresh tumor tissue and normal tissues were extracted protein and western blot was performed to identified the elevated expression in PC tissues compared with normal tissues. The statistics result of relative DDX31 expression to β-Tubulin western blot is shown in Fig. 3D. (E) The IHC stain of DDX31 in PDAC tissue paraffin section. Representative images are shown for weak, moderate, high expression of DDX31 in PDAC tissues. (×100 and ×200 magnification, Bar = 200 μm and 100μm) (F) The difference analysis of overall survival (OS) rate and progression-free survival (PFS) rate between DDX31 low (weakly expression and moderately expression) and high expression group. *: $p < 0.05$.

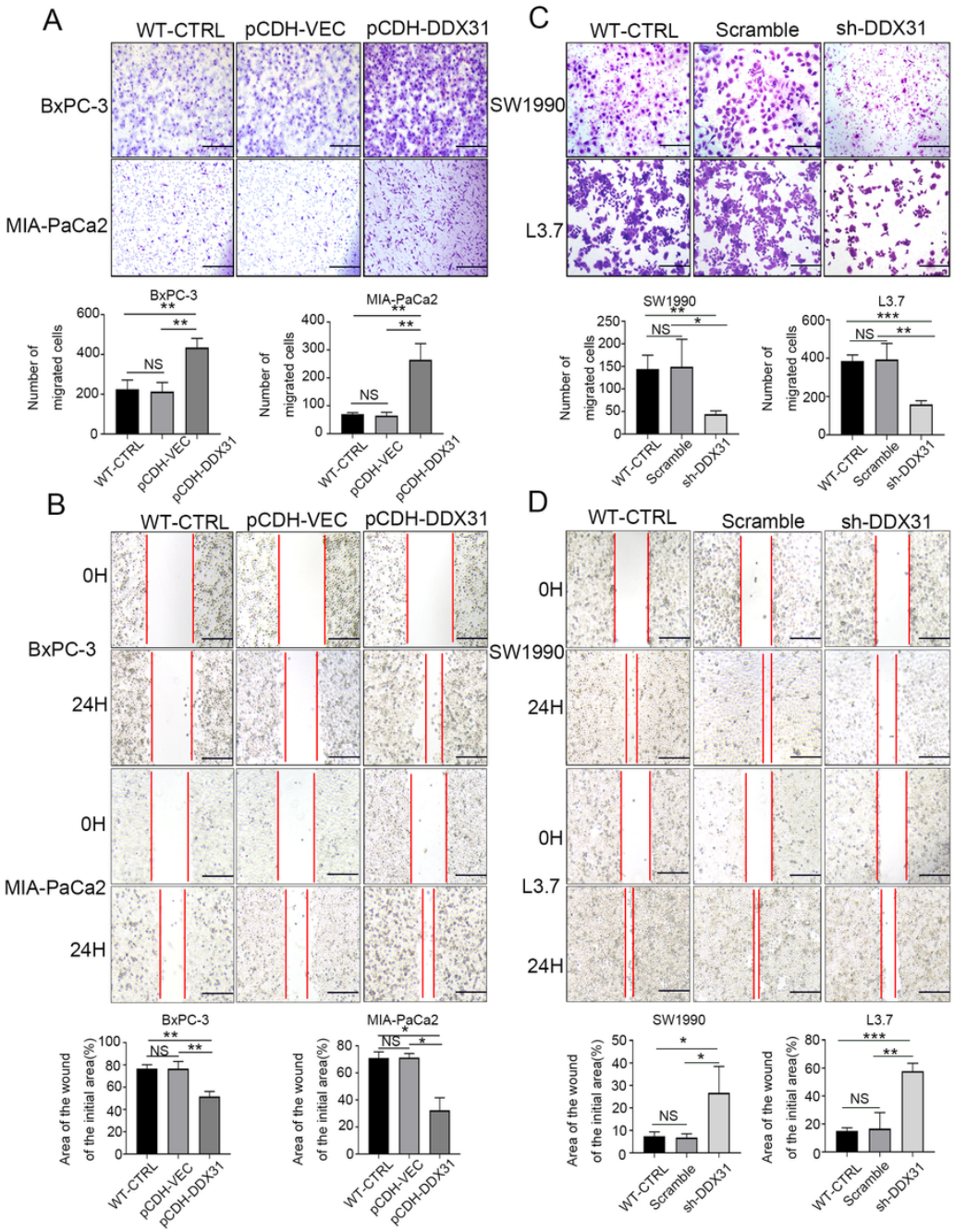

Figure 4

DDX31 promoted PC cell migration. (A) and (B) Cell migration was detected by transwell assays (Bar = 200 μm) and wound healing experiments (Bar = 200 μm) upon DDX31-overexpression PC cells lines BxPC-3 and MIA-PaCa2. (C) and (D) Transwell assay and wound healing assay were performed when DDX31 was downregulated in PC cells (SW1990 and L3.7). Images were collected three times randomly from each experiment (overexpression, left; knockdown, right). The figure at the bottom shows the corresponding statistical chart. (unpaired t-tests). Values are presented as the means ± SDs of three independent experiments. *: $p < 0.05$, **: $p < 0.01$, ***$p< 0.001$, ****$p< 0.0001$ and NS means non-significant.

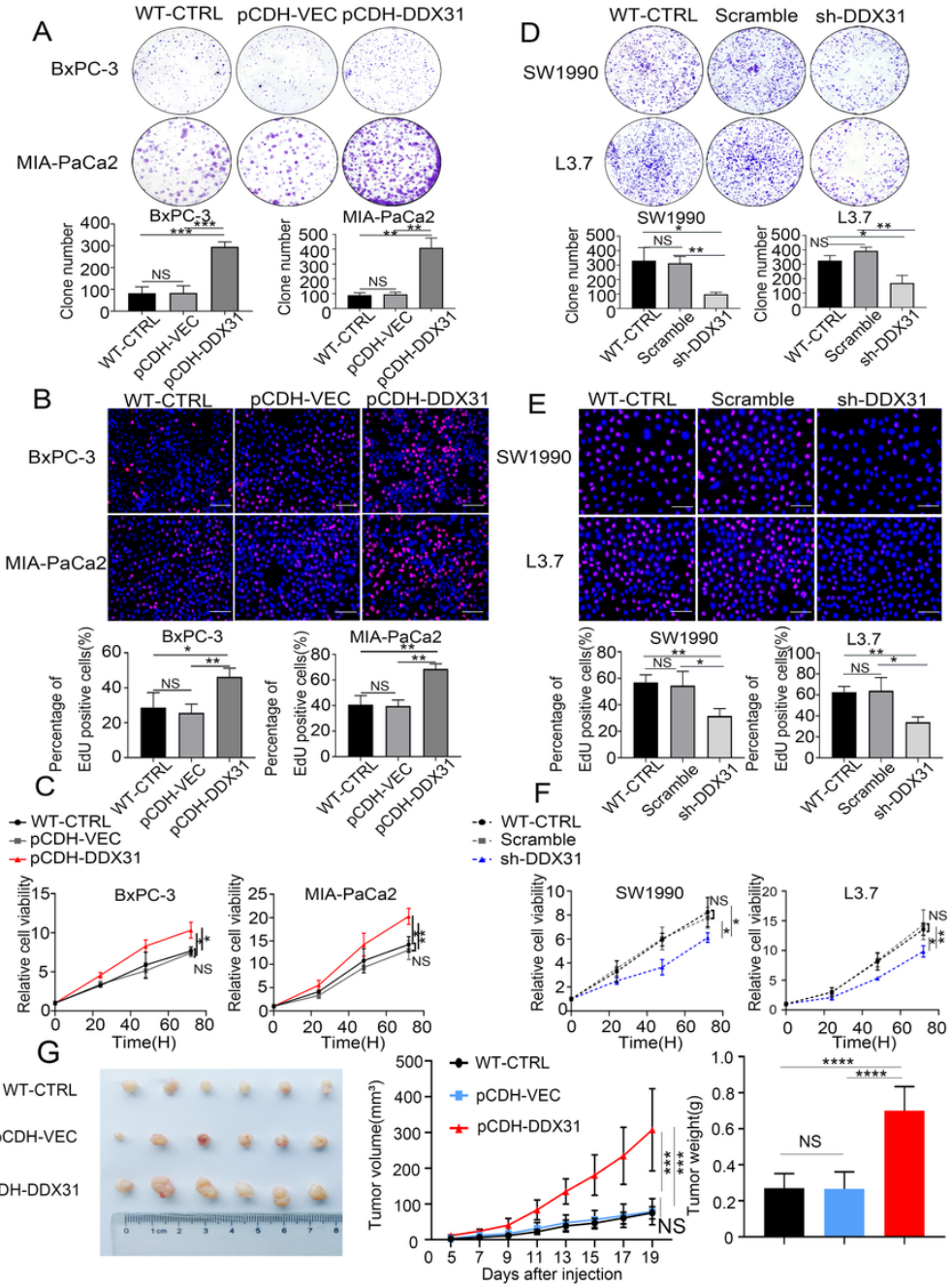

Figure 5

DDX31 promoted PC cell proliferation and cell viability. (A) and (D) Colony formation assays were performed in the indicated cell lines. Representative images and statistical analysis are shown (overexpression, left; knockdown, right). (B) and (E) EdU staining assays (Bar = 200 μm) were conducted in indicated cell lines. Representative images and statistical analysis are shown. (C) and (F) CCK-8 assays were performed to test the DDX31 function on cell viability in indicated cell lines. Representative growth curves are shown. (G) In vivo subcutaneous tumor model was used to determine the role of DDX31 on the cellular proliferation of BxPC-3 (infected with pCDH-DDX31 and pCDH-VECTOR lentivirus). Mice were sacrificed after 19 days; volume and mass of harvested tumors were measured 3 times a week. Each experiment was independently repeated three times, and representative results are shown. Unpaired Student's t test was used for A-G analysis. *p < 0.05, **p < 0.01 and NS means non-significant.

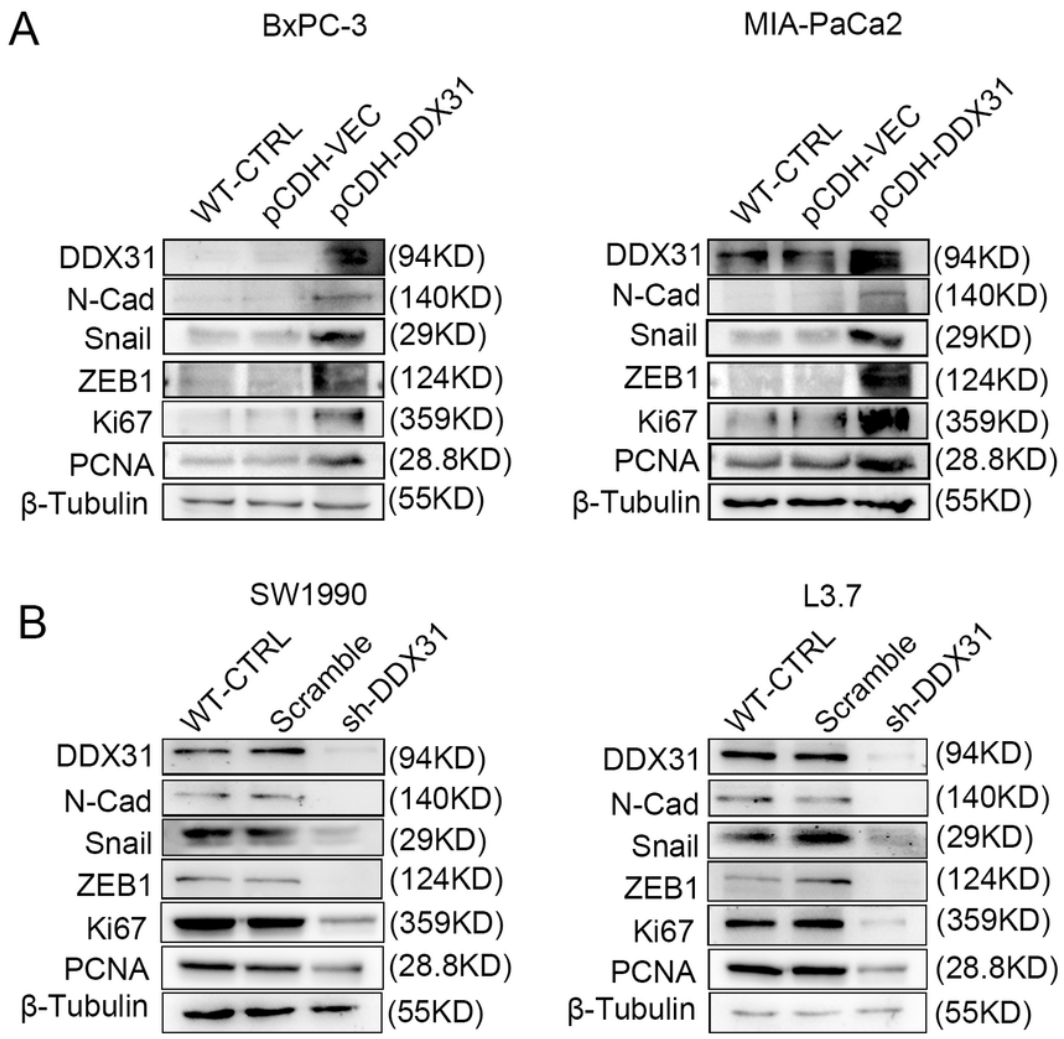

Figure 6

DDX31 was positively correlated with genes related to epithelial–mesenchymal transition and proliferation in PC cells. (A-B) Western blot was performed to confirm the relationship between DDX31 and N-cad, Snail, ZEB1, Ki67, and PCNA in BxPC-3/MiaPaCa-2-vector/DDX31-OE cell lines and SW1990/L3.7-vector/sh-DDX31 cell lines. β-Tubulin was used as loading control. Experiments were repeated three times, and representative results are shown.

Supplementary Files

This is a list of supplementary files associated with this preprint. Click to download.

- Supplementary1.png
- Supplementary2.png
- Supplementary3.png